ON SURFACE MESHES INDUCED BY LEVEL SET FUNCTIONS

MAXIM A. OLSHANSKII*, ARNOLD REUSKEN†, AND XIANMIN XU‡

Abstract. The zero level set of a continuous piecewise-affine function with respect to a consistent tetrahedral subdivision of a domain in $\mathbb{R}^3$ is a piecewise-planar hyper-surface. We prove that if a family of consistent tetrahedral subdivions satisfies the *minimum angle condition*, then after a simple postprocessing this zero level set becomes a consistent surface triangulation which satisfies the *maximum angle condition*. We treat an application of this result to the numerical solution of PDEs posed on surfaces, using a P_1 finite element space on such a surface triangulation. For this finite element space we derive optimal interpolation error bounds. We prove that the diagonally scaled mass matrix is well-conditioned, uniformly with respect to h. Furthermore, the issue of conditioning of the stiffness matrix is addressed.

Key words. surface finite elements, level set function, surface triangulation, maximum angle condition

1. Introduction. Surface triangulations occur in, for example, visualization, shape optimization, surface restoration and in applications where differential equations posed on surfaces are treated numerically. Hence, properties of surface triangulations such as shape regularity and angle conditions are of interest. For example, angle conditions are closely related to approximation properties and stability of corresponding finite elements [1, 2].

In this article, we are interested in the properties of a surface triangulation if one considers the zero level of a continuous piecewise-affine function with respect to a consistent tetrahedral subdivision of a domain in $\mathbb{R}^3$. The zero level of a piecewise-affine function is a piecewise-planar hyper-surface consisting of triangles and quadrilaterals. Each quadrilateral can be divided into two triangles in such a way that the resulting surface triangulation satisfies the following property proved in this paper: if the volume tetrahedral subdivision satisfies a minimum angle condition, then the corresponding surface triangulation satisfies a maximum angle condition. We show that the maximum angle occuring in the surface triangulation can be bounded by a constant $\phi_{\max} < \pi$ that depends only on a stability constant for the family of tetrahedral subdivisions.

The paper also discusses a few implications of this property for the numerical solution of surface partial differential equations. Numerical methods for surface PDEs are studied in e.g., [6, 4, 5, 3, 8, 10]. We derive optimal approximation properties of P_1 finite element functions with respect to the surface triangulation and a uniform bound for the condition number of the scaled mass matrix. We also show that the condition number of the (scaled) stiffness matrix can be very large and is sensitive to the distribution of the vertices of tetrahedra close to the surface. Some numerical examples illustrate the analysis of the paper.

2. Surface meshes induced by regular bulk triangulations. Consider a smooth surface Γ in three dimensional space. For simplicity, we assume that Γ is connected and has no boundary. Let $\Omega \subset \mathbb{R}^3$ be a bulk domain which contains

*Department of Mathematics, University of Houston, Houston, Texas 77204-3008 and Dept. Mechanics and Mathematics, Moscow State University, Moscow 119899 (molshan@math.uh.edu).

†Institut für Geometrie und Praktische Mathematik, RWTH-Aachen University, D-52056 Aachen, Germany (reusken@igpm.rwth-aachen.de).

‡LSEC, Institute of Computational Mathematics and Scientific/Engineering Computing, NCMIS, AMSS, Chinese Academy of Sciences, Beijing 100190, China (xmxu@lsec.cc.ac.cn).

Γ. Let $\{\mathcal{T}_h\}_{h>0}$ be a family of tetrahedral triangulations of the domain Ω. These triangulations are assumed to be regular, consistent and stable, cf. [2]. To simplify the presentation we assume that this family of triangulations is *quasi-uniform*. The latter assumption, however, is not essential for our analysis.

We assume that for each $\mathcal{T}_h$ an approximation of Γ, denoted by Γ_h, is given which is a connected $C^{0,1}$ surface without boundary. For a further analysis, we introduce the following definition.

DEFINITION 2.1. *For any tetrahedron $S_T \in \mathcal{T}_h$ such that* $\text{meas}_2(S_T \cap \Gamma_h) > 0$ *define $T = S_T \cap \Gamma_h$. If every T is a planar segment, then the surface approximation Γ_h is called* consistent with the outer triangulation *$\mathcal{T}_h$.*

If Γ_h is consistent with $\mathcal{T}_h$, then every segment $T = S_T \cap \Gamma_h$ is either a triangle or a quadrilateral. Each quadrilateral segment can be divided into two triangles, so we may assume that every T is a triangle.

Let $\mathcal{F}_h$ be the set of all triangular segments T, then Γ_h can be decomposed as

$$\Gamma_h = \bigcup_{T \in \mathcal{F}_h} T. \tag{2.1}$$

ASSUMPTION 2.1. *In the remainder of this paper we assume that Γ_h is a connected $C^{0,1}$ surface without boundary that is consistent with the outer triangulation $\mathcal{T}_h$.*

The most prominent example of such a surface triangulation is obtained in the context of level set techniques. Assume that Γ is represented as the zero level of a level set function ϕ and that ϕ_h is a continuous linear finite element approximation on the outer tetrahedral triangulation $\mathcal{T}_h$. Then if we define Γ_h to be the zero level of ϕ_h then Γ_h consists of piecewise planar segments and is consistent with $\mathcal{T}_h$. As an example, consider a sphere Γ, represented as the zero level of its signed distance function. For ϕ_h we take the piecewise linear nodal interpolation of this distance function on a uniform tetrahedral triangulation $\mathcal{T}_h$ of a domain that contains Γ. The zero level of this interpolant defines Γ_h and is illustrated in Fig. 2.1.

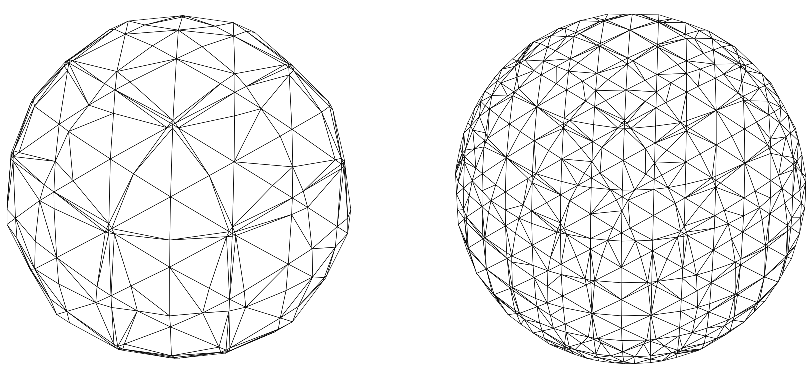

FIG. 2.1. *Approximate interface Γ_h for an example of a sphere, resulting from a coarse tetrahedral triangulation (left) and after one refinement (right).*

In the setting of level set methods, such surface triangulations induced by a finite element level set function on a regular outer tetrahedral triangulation are very natural and easy to construct. A surface triangulation Γ_h that is consistent with the outer triangulation may be the result of another method than the level set method. In the remainder we only need that Γ_h is consistent with the outer triangulation and not that it is generated by a level set technique.

Note that the triangulation $\mathcal{F}_h$ is *not* necessarily regular, i.e. elements $T \in \mathcal{F}_h$ may have *very small inner angles* and the *size of neighboring triangles can vary strongly*, cf. Fig. 2.1. In the next section we prove that, provided each quadrilateral is divided into two triangles properly, the induced surface triangulation is such that the *maximal angle condition* [1] is satisfied.

3. The maximal angle condition. The family of outer tetrahedral triangulations $\{\mathcal{T}_h\}_{h>0}$ is assumed to be regular, i.e., it contains no hanging nodes and the following stability property holds:

$$\sup_{h>0}\sup_{S\in\mathcal{T}_h} \rho(S)/r(S) \ \le\ \alpha < \infty, \tag{3.1}$$

where $\rho(S)$ and $r(S)$ are the diameters of the smallest ball that contains S and the largest ball contained in S, respectively. The stability property implies that the family of tetrahedral triangulations satisfies a *minimum* (and thus also maximum) *angle condition*: there exists $\theta_{\min} > 0$ with

$$\frac{\pi}{2} > \theta_{\min} \ge c(\alpha) > 0, \tag{3.2}$$

such that all inner angles of all sides of $S \in \mathcal{T}_h$ and all angles between edges of S and their opposite side are in the interval $[\theta_{\min}, \pi - \theta_{\min}]$. The constant $c(\alpha)$ depends only on α from (3.1).

Although the surface mesh Γ_h induced by $\mathcal{T}_h$ can be highly shape irregular, the following lemma shows that a *maximum angle* property holds.

LEMMA 3.1. *Assume an outer triangulation $\mathcal{T}_h$ from the regular family $\{\mathcal{T}_h\}_{h>0}$ and let Γ_h be consistent with $\mathcal{T}_h$. There exists $\phi_{\min} > 0$, depending only on α from* (3.1)*, such that for every $S \in \mathcal{T}_h$ the following holds:*

a) if $T = S \cap \Gamma_h$ is a triangular element, then

$$0 < \phi_{i,T} \le \pi - \phi_{\min} \quad i = 1, 2, 3, \tag{3.3}$$

holds, where $\phi_{i,T}$ are the inner angles of the element T.

b) if $T = S \cap \Gamma_h$ is a quadrilateral element, then

$$\phi_{i,T} \ge \phi_{\min}, \quad i = 1, 2, 3, 4, \tag{3.4}$$

holds, where $\phi_{i,T}$ are the inner angles of the element T.

Proof. Let $\theta_{\min}$ be the minimal angle bound from (3.2). Take $S \in \mathcal{T}_h$.

We first treat the case where $T = S \cap \Gamma_h$ is a triangle $T = BCD$, as illustrated in Fig. 3.1. Consider the angle $\phi := \angle BCD$. Then either $\phi \le \pi - \theta_{\min}$ and (3.3) is proved with $\phi_{\min} = \theta_{\min}$ or $\phi \in (\pi - \theta_{\min}, \pi)$. Hence, we treat the latter case. Note that

$$\frac{|CF|}{|AC|} = \sin(\angle CAF) \ge \sin\theta_{\min}$$

and $\angle BDC < \pi - \phi < \theta_{\min} < \frac{\pi}{2}$. Take E on the line through DB such that $CE \perp DB$, and F in the plane through ABD such that CF is perpendicular to this plane. Hence, $|CF| \le |CE|$ holds. Using the sine rule we get

$$\begin{aligned}\sin(\angle ADC) &= \frac{|AC|}{|CD|}\sin(\angle CAD) \le \frac{|AC|}{|CD|} \le \frac{1}{\sin\theta_{\min}}\frac{|CF|}{|CD|} \le \frac{1}{\sin\theta_{\min}}\frac{|CE|}{|CD|}\\ &= \frac{1}{\sin\theta_{\min}}\sin(\angle BDC) \le \frac{\sin(\pi-\phi)}{\sin\theta_{\min}} = \frac{\sin(\phi)}{\sin\theta_{\min}} < 1.\end{aligned}$$

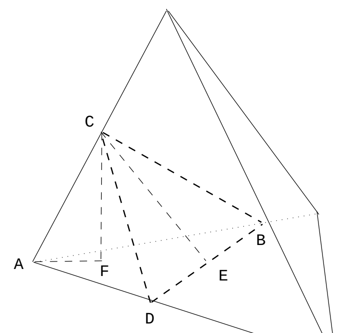

Fig. 3.1.

Hence, $\angle ADC \leq \arcsin(\frac{\sin\phi}{\sin\theta_{\min}}) \leq 2\frac{\sin\phi}{\sin\theta_{\min}}$ holds. This yields

$$\angle ADB < \angle ADC + \angle CDB \leq 2\frac{\sin\phi}{\sin\theta_{\min}} + \pi - \phi.$$

With the same arguments we obtain

$$\angle ABD \leq 2\frac{\sin\phi}{\sin\theta_{\min}} + \pi - \phi.$$

Since $\angle DAB \leq \pi - \theta_{\min}$ and $\angle DAB = \pi - (\angle ADB + \angle ABD)$ we get

$$\theta_{\min} \leq 4\frac{\sin\phi}{\sin\theta_{\min}} + 2\pi - 2\phi =: g(\phi). \tag{3.5}$$

Since $\phi \in (\pi - \theta_{\min}, \pi) \subset (\frac{1}{2}\pi, \pi)$ it suffices to consider $g(\phi)$ for $\phi \in (\frac{1}{2}\pi, \pi)$. Elementary computation yields $g(\frac{1}{2}\pi) > \theta_{\min}$, $g(\pi) = 0$ and g is monotonically decreasing on $(\frac{1}{2}\pi, \pi)$. Hence the inequality (3.5) holds iff $\phi \leq \phi_0$, where ϕ_0 is the unique solution in $(\frac{1}{2}\pi, \pi)$ of $g(\phi) = \theta_{\min}$. This proves the result in a).

We now consider the case where $T = S \cap \Gamma_h$ is a quadrilateral $T = ABCD$, as illustrated in Fig. 3.2. Consider the angle $\phi := \angle DAB$. Then either $\phi \in (0, \theta_{\min})$ or

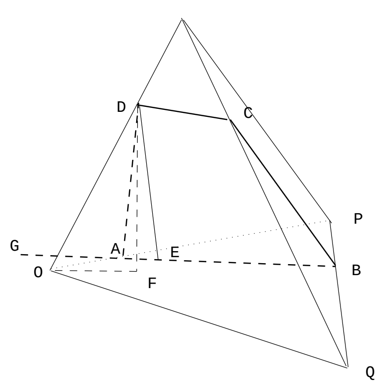

Fig. 3.2.

$\phi \in [\theta_{\min}, \pi)$. We only have to treat the former case. Take E on the line through AB

such that $DE \perp AB$, and F in the plane through OPQ such that DF is perpendicular to this plane. Hence, $|DF| \leq |DE|$ holds and

$$\sin\phi = \frac{|DE|}{|AD|}.$$

Furthermore, using $\frac{|DF|}{|OD|} = \sin(\angle DOF) \geq \sin\theta_{\min}$ we get

$$\begin{aligned}\sin(\angle OAD) &= \frac{|OD|}{|AD|}\sin(\angle AOD) \leq \frac{|OD|}{|AD|} \leq \frac{1}{\sin\theta_{\min}}\frac{|DF|}{|AD|} \\ &\leq \frac{1}{\sin\theta_{\min}}\frac{|DE|}{|AD|} = \frac{\sin\phi}{\sin\theta_{\min}} < 1.\end{aligned}$$

This implies

$$\angle OAD \leq \arcsin\big(\frac{\sin\phi}{\sin\theta_{\min}}\big) \leq 2\frac{\sin\phi}{\sin\theta_{\min}}.$$

Hence, since $\angle DAB = \phi \leq 2\sin\phi$, we obtain

$$\angle OAB < \angle OAD + \angle DAB \leq \big(1 + \frac{1}{\sin\theta_{\min}}\big)2\sin\phi.$$

Using $\angle OAB = \pi - \angle PAB$ and $\angle PAB < \pi - \angle OPQ < \pi - \theta_{\min}$ results in

$$\theta_{\min} < \big(1 + \frac{1}{\sin\theta_{\min}}\big)2\sin\phi. \tag{3.6}$$

For $\phi \in (0, \theta_{\min})$ the inequality (3.6) holds iff $\phi \geq \phi_0$, where ϕ_0 is the unique solution in $(0, \frac{1}{2}\pi)$ of $\theta_{\min} = \big(1 + \frac{1}{\sin\theta_{\min}}\big)2\sin\phi_0$. Thus the result in b) holds.
□

The lemma readily yields the following result.

THEOREM 3.2 (maximum angle condition). *Consider a regular family of tetrahedral triangulations $\{\mathcal{T}_h\}_{h>0}$ and a surface triangulation $\Gamma_h = \cup_{T\in\mathcal{F}_h} T$ that is consistent with $\mathcal{T}_h$. Assume that any quadrilateral element $T = S \cap \Gamma_h$, $S \in \mathcal{T}_h$, is divided in two triangles by connecting the vertex with largest inner angle with its opposite vertex. The resulting surface triangulation satisfies the following* maximal angle condition. *There exists $\phi_{\min} > 0$ depending only on α from* (3.1) *such that:*

$$0 < \sup_{T\in\mathcal{F}_h} \phi_{i,T} \leq \pi - \phi_{\min} \quad i = 1, 2, 3, \tag{3.7}$$

where $\phi_{i,T}$ are the inner angles of the element T.

Proof. If $T = S \cap \Gamma_h$ is a triangle, then (3.7) directly follows from (3.3). Let $T = S \cap \Gamma_h$ be a quadrilateral, with its four inner angles denoted by $\theta_4 \geq \theta_3 \geq \theta_2 \geq \theta_1 > 0$. From the result in (3.4) we have $\theta_i \geq \phi_{\min}$ for all i. The vertex with angle θ_4 is connected with the opposite vertex. Let T_1 be one of the resulting triangles. One of the angles of T_1 is θ_j with $j \in \{1, 2, 3\}$. From $\theta_j \geq \phi_{\min}$ it follows that the other two angles are both bounded by $\pi - \phi_{\min}$. Furthermore, from $\theta_j = 2\pi - \theta_4 - \sum_{i=1, i\neq j}^{3} \theta_i \leq 2\pi - \theta_j - 2\phi_{\min}$ it follows that $\theta_j \leq \pi - \phi_{\min}$ holds. □

In the remainder we assume that quadrilaterals are subdivided in the way as explained in Theorem 3.2. Hence, the inner angles in the surface triangulation $\mathcal{F}_h$ are bounded by a constant $\theta^* < \pi$ that depends only on the stability (close to Γ) of the outer tetrahedral triangulation $\mathcal{T}_h$. In particular θ^* is *independent of h and of how Γ_h intersects the outer triangulation $\mathcal{T}_h$.*

4. Application in a finite element method. In this section, we use the maximum angle property of the surface triangulation to derive an optimal finite element interpolation result. On $\mathcal{F}_h$ we consider the space of linear finite element functions:

$$V_h = \{v_h \in \mathcal{C}(\Gamma_h) : v_h \in \mathcal{P}_1(T) \quad \text{for all} \;\; T \in \mathcal{F}_h\}. \tag{4.1}$$

This finite element space is the same as the one studied by Dziuk in [5], but an important difference is that in the approach in [5] the triangulations have to be shape regular. In general, the finite element space V_h is different from the surface finite element space constructed in [8, 9].

Below we derive an approximation result for the finite element space V_h. Since the discrete surface Γ_h varies with h, we have to explain in which sense Γ_h is close to Γ. For this we use a standard setting applied in the analysis of discretization methods for partial differential equations on surfaces, e.g. [4, 5, 6, 7, 9].

Let $U := \{\, x \in \mathbb{R}^3 \mid \operatorname{dist}(x,\Gamma) < c\,\}$ be a sufficiently small neighborhood of Γ. We define $\mathcal{T}_h^\Gamma := \{\, T \in \mathcal{T}_h \mid \operatorname{meas}_2(T \cap \Gamma_h) > 0\,\}$, i.e., the collection of tetrahedra which intersect the discrete surface Γ_h, and assume that $\mathcal{T}_h^\Gamma \subset U$. Let d be the signed distance function to Γ, with $d < 0$ in the interior of Γ,

$$d : U \to \mathbb{R}, \qquad |d(x)| := \operatorname{dist}(x,\Gamma) \quad \text{for all } x \in U.$$

Thus Γ is the zero level set of d. Note that $\mathbf{n}_\Gamma = \nabla d$ on Γ. We define $\mathbf{n}(x) := \nabla d(x)$ for $x \in U$. Thus $\mathbf{n}$ is the outward pointing normal on Γ and $\|\mathbf{n}(x)\| = 1$ for all $x \in U$. Here and in the remainder $\|\cdot\|$ denotes the Euclidean norm on $\mathbb{R}^3$. We introduce a local orthogonal coordinate system by using the projection $\mathbf{p} : U \to \Gamma$:

$$\mathbf{p}(x) = x - d(x)\mathbf{n}(x) \quad \text{for all } x \in U.$$

We assume that the decomposition $x = \mathbf{p}(x) + d(x)\mathbf{n}(x)$ is unique for all $x \in U$. Note that $\mathbf{n}(x) = \mathbf{n}\big(\mathbf{p}(x)\big)$ for all $x \in U$. For a function v on Γ, its extension is defined as

$$v^e(x) := v(\mathbf{p}(x)), \quad \text{for all } x \in U. \tag{4.2}$$

The outward pointing (piecewise constant) unit normal on Γ_h is denoted by $\mathbf{n}_h$. Using this local coordinate system we introduce the following assumptions on Γ_h:

$$\mathbf{p} : \Gamma_h \to \Gamma \quad \text{is bijective}, \tag{4.3}$$

$$\max_{x \in \Gamma_h} |d(x)| \lesssim h^2, \tag{4.4}$$

$$\max_{x \in \Gamma_h} \|\mathbf{n}(x) - \mathbf{n}_h(x)\| \lesssim h, \tag{4.5}$$

where $h = \sup_{T \in \mathcal{T}_h^\Gamma} \rho(T)$. In (4.4)-(4.5) we use the common notation, that the inequality holds with a constant independent of h. In (4.5), only $x \in \Gamma_h$ are considered for which $\mathbf{n}_h(x)$ is well-defined. Using these assumptions, the following result is derived in [5].

LEMMA 4.1. *For any function $u \in H^2(\Gamma)$, we have, for arbitrary $T \in \mathcal{F}_h$ and $\tilde{T} := \mathbf{p}(T)$:*

$$\|u^e\|_{0,T} \simeq \|u\|_{0,\tilde{T}}, \tag{4.6}$$

$$|u^e|_{1,T} \simeq |u|_{1,\tilde{T}}, \tag{4.7}$$

$$|u^e|_{2,T} \lesssim |u|_{2,\tilde{T}} + h|u|_{1,\tilde{T}}, \tag{4.8}$$

where $A \simeq B$ means $B \lesssim A \lesssim B$ and the constants in the inequalities are independent of T and of h.

4.1. Finite element interpolation error. Based on the results in Lemma 4.1, the maximum angle property and the approximation results derived in [1] we easily obtain an optimal bound for the interpolation error in the space V_h. Consider the standard finite element nodal interpolation $I_h : C(\Gamma_h) \to V_h$:

$$(I_h v)(x) = v(x), \quad \text{for all} \quad x \in \mathcal{V}, \tag{4.9}$$

with $\mathcal{V}$ the set of vertices of the triangles in Γ_h.

THEOREM 4.2. *For any $u \in H^2(\Gamma)$ we have*

$$\|u^e - I_h u^e\|_{L^2(\Gamma_h)} \lesssim h^2 \|u\|_{H^2(\Gamma)}, \tag{4.10}$$

$$\|u^e - I_h u^e\|_{H^1(\Gamma_h)} \lesssim h \|u\|_{H^2(\Gamma)}. \tag{4.11}$$

Proof. From standard interpolation theory we have

$$\|u^e - I_h u^e\|_{L^2(T)} \lesssim h^2 |u^e|_{2,T},$$

where the constant in the upper bound is independent of (the shape of) T. Using the result in (4.8) and summing over $T \in \mathcal{F}$ proves the result (4.10). For the interpolation error bound in the H^1-norm we use the results from [1]. For the interpolation error bounds derived in that paper the maximum angle property is essential. From [1] we get

$$\|u^e - I_h u^e\|_{H^1(T)} \lesssim h \|u\|_{H^2(T)}.$$

Due to the maximum angle property the constant in the upper bound is independent of T. Using the results in Lemma 4.1 and summing over $T \in \mathcal{F}_h$ we obtain the result (4.11). □

If one considers an $H^1(\Gamma)$ elliptic partial differential equation on Γ, the error for its finite element discretization in the surface space V_h can be analyzed along the same lines as in [5]. A difference with the planar case is that geometric errors arise due to approximation of Γ by Γ_h. Using the interpolation error bounds in Theorem 4.2 and bounding the geometric errors, with the help of the assumptions (4.3)-(4.5), results in optimal order discretization error bounds.

4.2. Conditioning of the mass matrix. Clearly the (strong) shape irregularity of the surface triangulation will influence the conditioning of the mass and stiffness matrices. Let N be the number of vertices in the surface triangulation and $\{\phi_i\}_{i=1}^N$ the nodal basis of the finite element space V_h. The mass and stiffness matrices are given by

$$\mathbf{M} = (m_{ij})_{i,j=1}^N, \quad \text{with} \quad m_{ij} = \int_{\Gamma_h} \phi_i \phi_j \, ds, \tag{4.12}$$

$$\mathbf{A} = (a_{ij})_{i,j=1}^N, \quad \text{with} \quad a_{ij} = \int_{\Gamma_h} \nabla_{\Gamma_h} \phi_i \nabla_{\Gamma_h} \phi_j \, ds. \tag{4.13}$$

We also need their scaled versions. Let $\mathbf{D}_M$ and $\mathbf{D}_A$ be the diagonals of $\mathbf{M}$ and $\mathbf{A}$, respectively. The scaled matrices are denoted by

$$\mathbf{M}^s = \mathbf{D}_M^{-\frac{1}{2}} \mathbf{M} \mathbf{D}_M^{-\frac{1}{2}}, \quad \mathbf{A}^s = \mathbf{D}_A^{-\frac{1}{2}} \mathbf{A} \mathbf{D}_A^{-\frac{1}{2}}. \tag{4.14}$$

From a simple scaling argument it follows that the spectral condition number of $\mathbf{M}^s$ is bounded uniformly in h and in the shape (ir)regularity of the surface triangulation. For completeness we include a proof.

THEOREM 4.3. *The following holds:*

$$\frac{2}{\sqrt{2}+2} \leq \frac{\langle \mathbf{M}\mathbf{v}, \mathbf{v}\rangle}{\langle \mathbf{D}_M\mathbf{v}, \mathbf{v}\rangle} \leq 4 \quad \textit{for all} \ \ \mathbf{v} \in \mathbb{R}^N, \ \ \mathbf{v} \neq 0.$$

Proof. The set of all vertices in $\mathcal{F}_h$ is denoted by $\mathcal{V} = \{\, \xi_i \mid 1 \leq i \leq N \,\}$. Let $\mathbf{v} \in \mathbb{R}^N$ and $v_h \in V_h$ be related by $v_h = \sum_{i=1}^N v_i\phi_i$, i.e., $v_i = v_h(\xi_i)$. Consider a triangle $T \in \mathcal{F}_h$ and let its three vertices be denoted by ξ_1, ξ_2, ξ_3. Using quadrature we obtain

$$\begin{aligned}\int_T v_h(s)^2\, ds &= \frac{|T|}{3}\big(\frac{1}{4}(v_1+v_2)^2 + \frac{1}{4}(v_2+v_3)^2 + \frac{1}{4}(v_3+v_1)^2\big)\\ &= \frac{|T|}{6}\big(v_1^2 + v_2^2 + v_3^2 + v_1v_2 + v_2v_3 + v_3v_1\big).\end{aligned}$$

Hence, $\int_T v_h(s)^2\, ds \leq \frac{|T|}{3}\sum_{i=1}^3 v_i^2$ holds. From a sign argument it follows that at least one of the three terms v_1v_2, v_2v_3 or v_3v_1 must be positive. Without loss of generality we can assume $v_1v_2 \geq 0$. Using $|v_2v_3 + v_3v_1| \leq \frac{1}{\sqrt{2}}\big(v_1^2 + v_2^2 + v_3^2\big)$ we get

$$\int_T v_h(s)^2\, ds \geq \frac{|T|}{6}\big(v_1^2 + v_2^2 + v_3^2 - \frac{1}{\sqrt{2}}(v_1^2 + v_2^2 + v_3^2)\big) = \frac{|T|}{6(\sqrt{2}+2)}\big(v_1^2 + v_2^2 + v_3^2\big).$$

Note that $\langle \mathbf{M}\mathbf{v}, \mathbf{v}\rangle = \int_{\Gamma_h} v_h(s)^2\, ds = \sum_{T\in\mathcal{F}_h}\int_T v_h(s)^2\, ds$, and thus we obtain, with $\mathcal{V}(T)$ the set of the three vertices of T,

$$\frac{2}{\sqrt{2}+2}\frac{1}{12}\sum_{T\in\mathcal{F}_h}|T|\sum_{\xi\in\mathcal{V}(T)} v_h(\xi)^2 \leq \langle \mathbf{M}\mathbf{v}, \mathbf{v}\rangle \leq 4\frac{1}{12}\sum_{T\in\mathcal{F}_h}|T|\sum_{\xi\in\mathcal{V}(T)} v_h(\xi)^2. \tag{4.15}$$

We observe that

$$\frac{1}{12}\sum_{T\in\mathcal{F}_h}|T|\sum_{\xi\in\mathcal{V}(T)} v_h(\xi)^2 = \frac{1}{12}\sum_{i=1}^N |\mathrm{supp}(\phi_i)|v_i^2 \tag{4.16}$$

holds. From the definition of $\mathbf{D}_M$ it follows that

$$\begin{aligned}\langle \mathbf{D}_M\mathbf{v}, \mathbf{v}\rangle &= \sum_{i=1}^N \int_{\Gamma_h}\phi_i^2\, ds\, v_i^2 = \sum_{i=1}^N v_i^2 \sum_{T\in\mathrm{supp}(\phi_i)}\int_T \phi_i^2\, ds\\ &= \sum_{i=1}^N v_i^2 \sum_{T\in\mathrm{supp}(\phi_i)}\frac{|T|}{12} = \frac{1}{12}\sum_{i=1}^N |\mathrm{supp}(\phi_i)|v_i^2.\end{aligned} \tag{4.17}$$

Combination of the results in (4.15), (4.16) and (4.17) completes the proof. ∎

4.3. Conditioning of the stiffness matrix. We finally address the issue of conditioning of the diagonally scaled stiffness matrix $\mathbf{A}^s$, cf. (4.14). This matrix has a one dimensional kernel due to the constant nodal mode. Thus, we consider the effective condition number $\mathrm{cond}(\mathbf{A}^s) = \lambda_{\max}(\mathbf{A}^s)/\lambda_2(\mathbf{A}^s)$, where λ_2 is the minimal nonzero eigenvalue. We shall argue below that the condition number of $\mathbf{A}^s$ can not be bounded in general by a constant dependent exclusively on $\mathcal{T}_h$, but not on Γ_h. Indeed, assume a smooth closed surface Γ, with $|\Gamma| = 1$, and a smooth function u defined on Γ, such that $\|\nabla_\Gamma u\|_{L^2(\Gamma)} = \|u\|_{H^2(\Gamma)} = 1$. Let Γ_h be the zero level of the piecewise linear Lagrange interpolant of the signed distance function to Γ. Denote $u_h = I_h u^e$, as in Theorem 4.2, and $\mathbf{v} = (v_1, \ldots, v_N)^T$ is the corresponding vector of nodal values. From the result in (4.11) we obtain

$$\langle \mathbf{A}\mathbf{v}, \mathbf{v}\rangle = \|\nabla_{\Gamma_h} u_h\|_{L^2(\Gamma_h)} = 1 + O(h). \tag{4.18}$$

On the other hand, if there is a node ξ in the volume triangulation $\mathcal{T}_h$ such that $\mathrm{dist}(\xi, \Gamma_h) < \varepsilon \ll 1$, then there can appear a triangle in $\mathcal{F}_h$ with a minimal angle of $O(\varepsilon)$. This implies that there is a diagonal element in $\mathbf{A}$ of order $O(\varepsilon^{-1})$. Without lost of generality we may assume $A_{11} = O(\varepsilon^{-1})$ and $v_1 = 1$. Thus we get

$$\langle \mathbf{D}_A \mathbf{v}, \mathbf{v}\rangle \geq A_{11} v_1^2 = O(\varepsilon^{-1}). \tag{4.19}$$

Comparing (4.18) and (4.19) we conclude that $\mathrm{cond}(\mathbf{A}^s) \geq O(\varepsilon^{-1})$, with $\varepsilon \to 0$. Results of numerical experiments in the next section demonstrate that the blow up of $\mathrm{cond}(\mathbf{A}^s)$ can be seen in some cases.

One might also be interested in a more general dependence of the eigenvalues of $\mathbf{A}^s$ on the distribution of tetrahedral nodes in $\mathcal{T}_h$ in a neighborhood of Γ_h. To a certain extend this question is addressed in [8].

5. Numerical experiment. In this section we present a few results of numerical experiments which illustrate the interpolation estimates from Theorem 4.2 and the conditioning of mass and stiffness matrices. Assume the surface Γ, which is the unit sphere $\Gamma = \{\, x \in \mathbb{R}^3 \mid \|x\| = 1 \,\}$, is embedded in the bulk domain $\Omega = [-2, 2]^3$. The signed distance function to Γ is denoted by d. We construct a hierarchy of uniform tetrahedral triangulations $\{\mathcal{T}_h\}$ for Ω, with $h \in \{1/2, 1/4, 1/8, 1/16, 1/32\}$. Let d_h be the piecewise nodal Lagrangian interpolant of d. The triangulated surface is given by

$$\Gamma_h = \bigcup_{T \in \mathcal{F}_h} T = \{\, x \in \Omega \mid d_h(x) = 0 \,\}.$$

The corresponding finite element space V_h consists of all piecewise affine functions with respect to $\mathcal{F}_h$, as defined in (4.1). For $h \in \{1/2, 1/4, 1/8, 1/16, 1/32\}$, the resulting dimensions of V_h are $N = 164, 812, 3500, 14264, 57632$, respectively. In agreement with the 2D nature of Γ_h, we have $N \sim h^{-2}$.

To illustrate the result of Theorem 4.2, we present the interpolation errors $\|u^e - I_h u^e\|_{L^2(\Gamma_h)}$ and $|u^e - I_h u^e|_{1,\Gamma_h}$ for the smooth function

$$u(x) = \frac{1}{\pi} x_1 x_2 \arctan(2x_3)$$

defined on the unit sphere, with $x = (x_1, x_2, x_3)^T$. The dependence of the interpolation errors on the number of degrees of freedom N is shown in Figure 5.1 (left). We observe the optimal error reduction behavior, consistent with the estimates in (4.10), (4.11).

Further, for the same sequence of meshes we compute the spectral condition numbers of the mass matrix $\mathbf{M}$ and the diagonally scaled mass matrix $\mathbf{M}^s$. The dependence of the condition numbers on the number of degrees of freedom N is

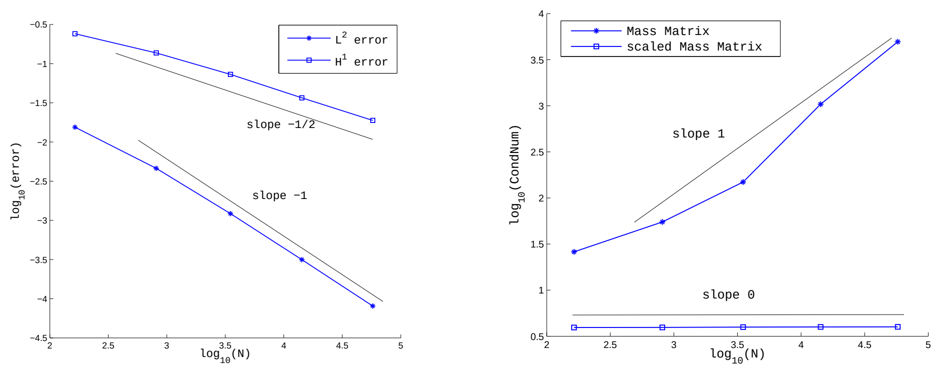

Fig. 5.1. *Left: Interpolation error as a function of # d.o.f.; Right: The condition number of the mass matrix as a function of of # d.o.f.*

illustrated in Figure 5.1 (right). As was proved in Theorem 4.3, the scaled mass matrix has a uniformly bounded condition number.

We discussed in section 4.3 that concerning the effective condition number of the scaled stiffness matrix the situation is more delicate. To illustrate this, we performed an experiment in which the intersection between a fixed outer triangulation and the surface is varied. Let Γ be the boundary of the unit sphere with the center located in $(0, 0, z_c)$. The discrete surface Γ_h is defined as described above, induced by the uniform outer triangulation. We choose a fixed outer triangulation with $h = 1/16$. We now consider different values for z_c, thus "moving the surface through the outer triangulation". The z_c values are given in the first column of Table 5.1. Note that for the largest shift $z_c = 0.03$ we have $z_c \approx 0.5h$.

For the different surface triangulations we computed the interpolation errors as described above. It turns out that for the values $z_c \neq 0$ the error behavior is essentially the same as that for $z_c = 0$, illustrated in the left subfigure in Fig. 5.1. Also the results for the condition number of the scaled mass matrix for the values $z_c \neq 0$ are essentially the same as those for $z_c = 0$, illustrated in the right subfigure in Fig. 5.1.

In the second to fourth columns of Table 5.1 two geometry related quantities are given. The second column shows the value of the maximum angle occuring in the surface triangulation. Consistent to the theory, cf. Theorem 3.2, the maximum angle is bounded away from 180°. Small angles, however, can occur. In the third and fourth column we show the value of the minimum angle and the number of triangles in the surface triangulation with the smallest angle smaller than 1°. As expected, both the minimal angle and this number of small angles strongly vary, depending on z_c. For $z_c = 0$ the smallest angle in the surface triangulation has value $\phi_{\min} = 1.9°$. Extremely small angles can occur, e.g. for $z_c = 0.00005$, we have $\phi_{\min} = 8.5\text{e-}7°$. The dimension and the effective condition number of the scaled stiffness matrix $\mathbf{A}^s$ are given in the fifth and sixth column of Table 5.1. The values of the condition number show a strong dependence on the sphere location (value of z_c). These large condition numbers indicate that linear systems with these matrices may be hard to solve using an iterative method.

The topic of efficient solvers for systems of linear algebraic equations resulting from discretization on the surface meshes is outside the scope of this paper. We restrict ourselves to the presentation of a few results of numerical experiments with the scaled stiffness matrix for the example described above. For the purpose of comparison, we also construct a reference matrix $\mathbf{A}^{\mathrm{ref}}$ as follows: $\mathbf{A}^{\mathrm{ref}} = \text{blocktridiag}(-\mathbf{B}^T, \mathbf{D}, -\mathbf{B})$, with $\mathbf{D} = \text{tridiag}(-1, 6, -1)$, $\mathbf{B} = \text{tridiag}(0, 1, 1)$. In most rows the matrix $\mathbf{A}^{\mathrm{ref}}$ has 7 nonzero entries, which is approximately the same as the average number of nonzero entries per row in the matrix $\mathbf{A}^s$ used in the experiment. In $\mathbf{A}^{\mathrm{ref}}$ we use 120 blockrows and blockcolums and the matrices $\mathbf{D}$ and $\mathbf{B}$ have dimension 120. Then the matrix $\mathbf{A}^{\mathrm{ref}}$ has dimension 14400, which is comparable to the dimension of $\mathbf{A}^s$ used in the experiment, cf. Table 5.1.

First we study the performance of an iterative solver. We use the standard PCG MATLAB solver with ILU(0) preconditioner. For given $\mathbf{v}$, we compute $\mathbf{b} = \mathbf{A}^s\mathbf{v}$ and apply the MATLAB PCG iterative solver with a relative residual tolerance of 10^{-8}. The resulting iteration numbers are given in column 7 of Table 5.1. The same iterative solver with the same stopping criterion applied to a linear system with $\mathbf{A}^{\mathrm{ref}}$ results in only 42 PCG iterations.

Solving a PDE on a surface (in 3D) is a *two*-dimensional problem, therefore a sparse direct solver may be a competitive alternative to an iterative method. We performed experiments with the MATLAB sparse direct solver $\mathbf{A}^s \setminus \mathbf{b}$. We measure computing time by the MATLAB function CPUTIME. For the system with the reference matrix $\mathbf{A}^{\mathrm{ref}}$ we obtained (on our machine) CPUTIME= 1.38. For the matrix $\mathbf{A}^s$ and the values for z_c as in the first column of Table 5.1 we obtained CPU time measurements that varied between 1.43 and 3.64. These time measurements indicate that for the direct MATLAB solver the matrices $\mathbf{A}^s$ are not (much) more difficult to deal with than the reference matrix $\mathbf{A}^{\mathrm{ref}}$. Variations in CPU times are likely caused by slightly different fill-in properties of matrices for different grids. The one dimensional kernel of the matrix $\mathbf{A}^s$ did not cause difficulties for the solver. We checked the accuracy of the computed solution (in the energy norm) and this was satisfactory.

We conclude that in this particular example the systems with $\mathbf{A}^s$ are signifantly more expensive to solve with the standard ILU(0) preconditioned CG method than a system with the reference matrix. The sparse direct solver does not show such a strong decrease in efficiency if instead of a system with the reference matrix a system with the scaled stiffness matrix $\mathbf{A}^s$ is solved.

z_c	$\phi_{\max}$	$\phi_{\min}$	$\#T$: $\phi_{\min}<1^\circ$	$\dim(\mathbf{A}^s)$	$\text{cond}(\mathbf{A}^s)$	# PCG
0.03	147.4°	0.050°	420	14406	1.82e+4	245
0.02	145.3°	0.027°	292	14376	2.20e+4	282
0.008	145.4°	0.014°	270	14368	3.44e+4	331
0.002	144.3°	0.002°	126	14300	1.94e+5	285
0.0005	141.0°	1.22e-4°	20	14288	3.07e+6	259
0.00025	140.4°	3.05e-5°	20	14288	1.23e+7	191
0.00005	139.9°	8.54e-7°	24	14288	3.06e+8	202
0	139.8°	1.85°	0	14264	9.14e+3	142

TABLE 5.1

Angles in the surface triangulation, dimension of $\mathbf{A}^s$, $\text{cond}(\mathbf{A}^s)$, *iteration count for PCG and timing for direct solver.*

6. Conclusions. The main new result of this paper is a geometric property of the piecewise planar surface which is the zero level of a continuous piecewise affine level set function. If this piecewise planar surface is consistent with an outer tetrahedral triangulation that satisfies the *minimum angle condition*, then after a suitable subdivision of the quadrilaterals into two triangles the resulting surface triangulation satisfies a *maximum angle condition*. This maximum angle property of the surface triangulation is used to derive optimal error bounds for the nodal interpolation operator in the finite element space of continuous piecewise linear functions on the surface triangulation. This implies that the discretization of a surface diffusion PDE in this finite element space results in optimal discretization error bounds. We study the conditioning of the scaled mass and stiffness matrices corresponding to this finite element space. The condition number o! f the sca led mass matrix is shown to be uniformly bounded. The scaled stiffness matrix can have a very large effective condition number. A topic that we plan to investigate further is whether some grid smoothing (elimination of extremely small angles) can be developed such that the optimal approximation property still holds and the conditioning of the scaled stiffness matrix is improved.

Acknowledgments. The authors thank the referees for their comments, which led to significant improvements of the original version of this paper. This work has been supported in part by the DFG through grant RE1461/4-1 and the Russian Foundation for Basic Research through grants 12-01-91330, 12-01-00283, 12-01-33084.

REFERENCES

[1] I. Babuška and A. K. Aziz. On the angle condition in the finite element method. *SIAM J. Numer. Anal.*, 13:214–226, 1976.

[2] P. Ciarlet. *The Finite Element Method for Elliptic Problems.* North-Holland, Amsterdam, 1978.

[3] A. Demlow. Higher-order finite element methods and pointwise error estimates for elliptic problems on surfaces. *SIAM J. Numer. Anal.*, 47:805–827, 2009.

[4] A. Demlow and G. Dziuk. An adaptive finite element method for the Laplace-Beltrami operator on implicitly defined surfaces. *SIAM J. Numer. Anal.*, 45:421–442, 2007.

[5] G. Dziuk. Finite elements for the Beltrami operator on arbitrary surfaces. In S. Hildebrandt and R. Leis, editors, *Partial differential equations and calculus of variations*, volume 1357 of *Lecture Notes in Mathematics*, pages 142–155. Springer, 1988.

[6] G. Dziuk and C. Elliott. Finite elements on evolving surfaces. *IMA J. Numer. Anal.*, 27:262–292, 2007.

[7] G. Dziuk and C. Elliott. L^2-estimates for the evolving surface finite element method. *Math. Comp.*, 82:1–24, 2013.

[8] M. A. Olshanskii and A. Reusken. A finite element method for surface PDEs: matrix properties. *Numer. Math.*, 114:491–520, 2009.

[9] M. A. Olshanskii, A. Reusken, and J. Grande. A finite element method for elliptic equations on surfaces. *SIAM J. Numer. Anal.*, 47:3339–3358, 2009.

[10] J.-J. Xu and H.-K. Zhao. An Eulerian formulation for solving partial differerential equations along a moving interface. *J. Sci. Comput.*, 19:573–594, 2003.